Available online at www.sciencedirect.com
SCIENCE DIRECT®
International Journal of Solids and Structures 42 (2005) 1681–1704
INTERNATIONAL JOURNAL OF SOLIDS and STRUCTURES
www.elsevier.com/locate/ijsolstr

Numerical limit analysis solutions for the bearing capacity factor N_γ

M. Hjiaj *,[1], A.V. Lyamin, S.W. Sloan

Department of Civil Surveying and Environmental Engineering, The University of Newcastle, University Drive, Callaghan NSW 2308, Australia

Received 23 January 2004; received in revised form 5 August 2004
Available online 8 October 2004

Abstract

Numerical limit analyses are applied to evaluate the self-weight bearing capacity factor for a rigid surface footing with a smooth or rough interface. To isolate the effect of the self-weight on the bearing capacity, the soil is modeled as a cohesionless frictional Mohr–Coulomb material. Assuming an associated flow rule, the true collapse load is bracketed to within 3.42% by computing rigorous lower and upper bound solutions using recently developed limit analysis methods [Lyamin and Sloan, 2002a. Upper bound limit analysis using linear finite elements and non-linear programming. International Journal for Numerical and Analytical Methods in Geomechanics 26 (2), 181; Lyamin and Sloan, 2002b. Lower bound limit analysis using linear finite elements and non-linear programming. International Journal for Numerical Methods in Engineering 55 (5), 573]. With these sharp bounds, the average bearing capacity factor provides an excellent estimate of the exact bearing capacity factor that can be used with confidence for design purposes. The numerical formulations of both the upper and the lower bound theorems are obtained by means of finite elements and solved using efficient non-linear mathematical programming schemes. The solutions, presented in the form of graphs, are compared against existing semi-empirical expressions and numerical solutions. An approximate analytical expression for N_γ is suggested at the end of the paper.

Keywords: Bearing capacity factor; Self-weight; Cohesionless frictional material; Limit analysis; Finite element method

* Corresponding author. Tel.: +61 2 49 21 55 82; fax: +61 2 49 21 69 91.
E-mail address: mohammed.hjiaj@newcastle.edu.au (M. Hjiaj).
[1] Supported by the Australian Research Council.

0020-7683/$ - see front matter © 2004 Elsevier Ltd. All rights reserved.
doi:10.1016/j.ijsolstr.2004.08.002

1. Introduction

The bearing capacity of a shallow strip footing is generally determined by the Terzaghi method (Terzaghi, 1943). Terzaghi's equation is based on an approximate solution which uses superposition to combine the effects of cohesion, surcharge, and soil weight. The resulting bearing capacity equation is typically written in the form:

$$q_u = cN_c + qN_q + \frac{1}{2}\gamma B N_\gamma \tag{1}$$

where the bearing capacity factors N_c, N_q and N_γ represent the effects of soil cohesion c, surcharge q, and soil unit weight γ, respectively, and B is the width of the strip footing. These bearing capacity factors are all functions of the internal friction angle ϕ. Terzaghi's assumption of superposition, although widely used, is questionable since soil behavior in the plastic range is non-linear. The theoretical justification for using this principle has been investigated by Davis and Booker (1971). Their work suggests that the use of superposition, although not rigorous, leads to conservative estimates of the ultimate bearing capacity and will therefore result in a "safe" design.

The use of superposition simplifies the mathematical analysis considerably and, because of the complications that are introduced by the inclusion of self-weight, the general bearing capacity problem is usually solved in two stages. In the first stage, the analytical solution of Prandtl (1921), which assumes a weightless material, is used to give the bearing capacity factors N_c and N_q in closed form. In the second stage, the contribution of the soil weight is typically found using a numerical solution technique to give the bearing capacity factor N_γ.

While the exact values for N_γ remain unknown, the values for N_c and N_q, as given by Prandtl (1921), and Reissner (1924) are exact for a strip footing on a weightless soil. As discussed by Chen (1975), the analysis of cohesionless soil with self-weight is complicated by the fact that the shear strength increases with depth from a value of zero at the ground surface. This means that the Prandtl failure mechanism is no longer capable of yielding exact results, since any velocity discontinuity that is initially straight for the weightless case now becomes curved. This leads to the conclusion that the bearing capacity obtained using this mechanism can, at best, only be an upper bound on the correct value. Similar conclusions may be drawn regarding the mechanism suggested by Hill (1949).

In addition to the upper bounds obtained from the Hill and Prandtl mechanisms, various slip-line solutions have also been developed for the bearing capacity of a cohesive-frictional soil with weight. Slip-line methods use a variety of numerical schemes (finite difference, perturbation techniques, series expansion) to integrate the hyperbolic set of partial differential equations which describe the plastic stress field at equilibrium. Indeed, it has been shown by Booker (1969) that these characteristic equations must be integrated numerically if soil weight is included in the analysis. The numerical solution of characteristic equations is described in detail by Sokolovskii (1965). If an associated flow rule is used, and the resulting stress-strain rate equations can be integrated to yield a kinematically admissible velocity field, the slip-line solution is an upper bound solution. If, in addition, the slip-line stress field can be extended over the entire soil domain such that the equilibrium equations, the stress boundary conditions and the yield condition are satisfied, the slip-line solution is also a lower bound, and is hence the exact solution. Although the slip-line method may be used to compute a partial plastic stress field, there is no guarantee that this stress field can be associated with a kinematically admissible velocity field or extended satisfactorily throughout the body (Bishop, 1953). Although the slip-line method can generally be expected to give a good estimate of the correct solution, its accuracy is difficult to ascertain once either of the bounding properties is lost.

Due to the complexities that are associated with the introduction of self-weight, a great variety of approximate solutions for the bearing capacity factor N_γ have appeared in the literature (Chen, 1975).

The differences among these solutions is often very substantial, particularly for friction angles greater than about 30°. Unfortunately, experimental research on the ultimate bearing capacity of footings on sand has not shed much light on the question of which values of N_γ are theoretically correct. This is partly because of the difficulty in selecting an appropriate friction angle for the bearing capacity calculations when comparing the theoretical predictions with test results. Scale effects are also another complication. Existing theoretical solutions suggest that the factor increases very rapidly with the angle of friction. In view of this strong dependence, it seems unlikely that footing experiments alone can resolve the question of which values of N_γ are correct.

For elastic-perfectly plastic materials with an associated flow rule, Drucker et al. (1952) developed upper and lower bound limit theorems that can be used to bracket the true ultimate load from above and below. Generally speaking, the upper bound theorem is applied more frequently than the lower bound theorem to predict soil collapse. This is because it is considerably easier to construct a good kinematically admissible failure mechanism than it is to construct a good statically admissible stress field. Although an upper bound solution is often a good estimate of the collapse load, a lower bound solution is more valuable in engineering practice as it results in a safe design. The bound theorems are especially powerful when both types of solution can be computed so that the actual collapse load can be bracketed from above and below. Due to the obvious difficulties in constructing a good statically admissible stress field for a strip footing on ponderable cohesionless soil, the writers are unaware of any rigorous lower bound solution for the bearing capacity factor N_γ. Reasonable upper bound solutions, however, have been presented using both the Hill and Prandtl mechanisms and are discussed at length in Chen (1975). More recently, Michałowski (1997) and Soubra (1998), among others, have used rigid-block mechanisms to estimate the bearing capacity factor N_γ. Their results show some improvement on Chen's solutions but are still fairly conservative.

The last three decades has witnessed a growing use of the finite element method in almost all areas of geotechnical engineering, including shallow foundation stability. However only a few authors have attempted to apply this method to predict the bearing capacity of strip footings on cohesionless soils (Sloan and Randolph, 1982; Griffiths, 1982; Frydman and Burd, 1997). This is largely due to the difficulty in developing finite element formulations that are capable of providing precise estimates of the limit load.

In this paper, rigorous bounds are obtained for the bearing capacity factor N_γ by using two numerical techniques which are based on the limit theorems of classical plasticity and finite elements. The solutions presented in this paper extend the previous work of the authors (Hjiaj et al., 2003) and are compared with those obtained by other investigators. The methods assume a rigid plastic soil model with a Mohr–Coulomb yield criterion and lead to non-linear programming problems. In order to isolate the bearing capacity contribution of the N_γ term, the contributions of the other two terms in Eq. (1) are eliminated by assuming the soil to be cohesionless with zero surcharge. The solution to the kinematic optimization problem defines a kinematically admissible velocity field and gives a rigorous upper bound on the bearing capacity. The solution to the static optimization problem defines a statically admissible stress field and results in a rigorous lower bound on the bearing capacity. For internal friction angles ranging from 5° to 45°, the upper and lower bound solutions for N_γ differ from their mean by less than 3.42%. Thus the new bounding results are sufficiently accurate for the purposes of design.

The rest of the paper is organized as follows. Section 2 defines the problem under consideration, describes the governing equations, and introduces the notation used. In Section 3, the limit analysis theorems are briefly recalled and the mathematical programming problems obtained after discretization are presented in Section 4. Section 5 summarizes previous contributions according to the method used, including the widely used semi-empirical expressions developed by Meyerhof, Hansen and Vesić. Numerical results are given in Section 6 and compared with previous N_γ estimates. A new analytical expression for N_γ is also suggested.

2. Problem definition

The present study deals with the determination of the bearing capacity factor stemming from the self-weight of the soil. We consider a rigid strip footing of width B, resting on a deep homogenous soil of unit weight γ. The foundation is subjected to a vertical load at its centerline (Fig. 1). The length of the footing, denoted by L, is supposed to be large enough such that a condition of plane strain will exist in the soil mass supporting the foundation. Both rough and smooth interfaces between the footing and the soil mass are considered. The soil is assumed to be rigid perfectly plastic and modeled by a Mohr–Coulomb yield criterion with friction angle ϕ. By considering the case of zero surcharge and zero soil cohesion, the N_γ term can be estimated directly using limit analysis.

The solution of a limit analysis problem involves the determination of the limit load multiplier μ, a statically admissible stress field, and a kinematically admissible velocity field where the stress and the plastic strain rate fields are related by the flow rule. Since our interest is directed towards incipient failure, all equations may be referred to the original, undeformed state. In the next subsection, we specify the requirements that need to be satisfied by the stress and velocity fields with reference to the problem under consideration. Concerning the notation, both vectors and matrix are in bold face. The superimposed dot denotes a time-derivative and the scalar product is represented by "·".

2.1. Static admissibility

A stress field is said to be *statically admissible* if it satisfies the local equilibrium equations within the domain Ω (corresponding to a half-space) and on its boundary and does not violate the plastic yield criterion. Under plane strain conditions, the equilibrium equations within the domain Ω are

$$\frac{\partial \sigma_x}{\partial x} + \frac{\partial \tau_{xy}}{\partial y} = 0 \tag{2}$$

$$\frac{\partial \tau_{xy}}{\partial x} + \frac{\partial \sigma_y}{\partial y} = \gamma \tag{3}$$

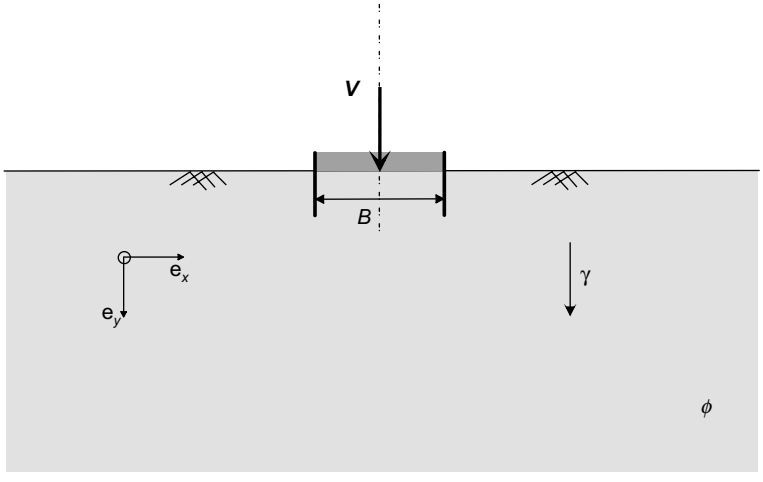

Fig. 1. Strip footing resting on a cohesionless, ponderable soil.

where σ_x, σ_y and τ_{xy} are the in-plane components of the Cauchy stress tensor. For a rigid foundation, the normal component of the surface tractions underneath the footing needs to equilibrate the applied vertical load

$$\mu^s V = -\int_{-0.5B}^{0.5B} \sigma_y \, \mathrm{d}x \tag{4}$$

where μ^s is a static load multiplier corresponding to the stress field considered. For a rough soil-foundation interface, the distribution of the shear tractions should lead to a null horizontal resultant

$$\int_{-0.5B}^{0.5B} \tau_{xy} \, \mathrm{d}x = 0 \tag{5}$$

If the footing is smooth, the relation (5) has to be replaced by the following point-wise condition

$$\tau_{xy} = 0, \quad \forall x \in \left[-\frac{B}{2}, \frac{B}{2}\right] \quad \text{and} \quad y = 0 \tag{6}$$

With no surcharge, the stress field needs to satisfy

$$\boldsymbol{n}, \boldsymbol{\sigma} = \mathbf{0} \tag{7}$$

where $\boldsymbol{n}$ denotes an operator composed of the components of the outward normal to the free surface. The last requirement to be fulfilled by the stress field is to lie within the yield locus:

$$f(\boldsymbol{\sigma}) \leqslant 0 \tag{8}$$

where $f(\boldsymbol{\sigma})$ is the Mohr–Coulomb yield criterion for cohesionless soil and plane strain loading

$$f(\boldsymbol{\sigma}) = (\sigma_x - \sigma_y)^2 + 4\tau_{xy}^2 - (\sin\phi(\sigma_x + \sigma_y))^2 \tag{9}$$

Here we adopt the solid mechanics convention where tensile normal stresses are taken as positive. Any stress field $\boldsymbol{\sigma}^{sa}$ satisfying (2)–(4), (5) or (6), (7) and (8) is said to be statically admissible. We denote by $\mathscr{S}_{ad}$ the space of all statically admissible stress fields.

2.2. Kinematic admissibility

A velocity field is said to be *kinematically admissible* if it satisfies the kinematic relations relating velocity and strain rate, the velocity boundary conditions, the flow rule, and leads to a positive value of the power generated by the external loads. For plane strain problems, the kinematic equations relating velocity and strain rate in a small displacement setting are

$$\dot{\varepsilon}_x^p = \frac{\partial v_x}{\partial x}, \quad \dot{\varepsilon}_y^p = \frac{\partial v_y}{\partial y}, \quad \dot{\varepsilon}_{xy}^p = \frac{1}{2}\left(\frac{\partial v_x}{\partial y} + \frac{\partial v_y}{\partial x}\right), \quad \dot{\varepsilon}_z^p = 0 \quad \text{in } \Omega \tag{10}$$

where $\dot{\varepsilon}_x^p$, $\dot{\varepsilon}_y^p$, $\dot{\varepsilon}_z^p$ and $\dot{\varepsilon}_{xy}^p$ are the components of the plastic strain rate tensor and v_x and v_y are the components of the velocity vector. The vertical rigid body motion of the footing imposes vertical velocity constraints at points along the interface. If we denote the velocity of the footing center by $\mathbf{v}^c$

$$\mathbf{v}^c = v_y^c, \mathbf{e}_y$$

then the boundary conditions are

$$\text{rough}: \quad v_y = v_y^c \quad \text{and} \quad v_x = 0, \quad \forall x \in \left[-\frac{B}{2}, \frac{B}{2}\right] \text{ and } y = 0 \tag{11}$$

$$\text{smooth}: \quad v_y = v_y^c \quad \text{and} \quad v_x \neq 0, \quad \forall x \in \left[-\frac{B}{2}, \frac{B}{2}\right] \text{ and } y = 0 \tag{12}$$

In addition, far away from the footing the soil remains rigid and the velocity is taken equal to zero. For an associated flow rule, the direction of the plastic strain rate is given by the gradient to the yield function and its magnitude by the plastic multiplier:

$$\dot{\boldsymbol{\varepsilon}}^p = \dot{\lambda}\frac{\partial f}{\partial \boldsymbol{\sigma}} \tag{13}$$

To ensure that this gradient exists everywhere, a smooth version of the original Mohr–Coulomb criterion is used (Abbo and Sloan, 1995). By definition, the power expended by the external forces in any kinematically admissible velocity field is given by

$$\mathscr{P}_e(\mathbf{v}) = \mu^k V, v_y^c + \int_\Omega \gamma v_y \,\mathrm{d}\Omega \tag{14}$$

and must be positive: $\mathscr{P}_e(\mathbf{v}) > 0$. By introducing the following notation

$$\langle v_y \rangle = \int_\Omega v_y \,\mathrm{d}\Omega$$

and assuming that γ is uniform, (14) can be rewritten as

$$\mathscr{P}_e(\mathbf{v}) = \mu^k V, v_y^c + \gamma\langle v_y \rangle > 0 \tag{15}$$

Any velocity field complying with the conditions (10), (11) or (12), (13) and (15) is kinematically admissible and the space encompassing all such fields is denoted by $\mathscr{V}_{ad}$. A major feature of limit analysis is the presence of discontinuities in both the velocity and stress fields. Physically, a velocity discontinuity corresponds to an intense distortion in the deformation field. The total rate of internal dissipation in any kinematically admissible velocity field is computed by summing the rate of dissipation that occurs due to plastic deformation and the rate of dissipation along the velocity discontinuities:

$$\mathscr{P}_i(\mathbf{v}) = \int_\Omega \boldsymbol{\sigma}\cdot\dot{\boldsymbol{\varepsilon}}^p \,\mathrm{d}\Omega + \int_{\mathscr{D}} (\boldsymbol{n},\boldsymbol{\sigma})\cdot[\![\mathbf{v}]\!]\,\mathrm{d}\Gamma \tag{16}$$

In the above, $\mathscr{D}$ represents any line of discontinuity in the velocity field and $[\![\mathbf{v}]\!]$ is the velocity discontinuity:

$$[\![\mathbf{v}]\!] = \mathbf{v}^+ - \mathbf{v}^- \tag{17}$$

where $\mathbf{v}^+$ and $\mathbf{v}^-$ represent the velocity on both sides of the discontinuity and $\boldsymbol{n}$ is the outward normal operator to $\mathscr{D}$. For a cohesionless frictional material with an associated flow rule, the rate of the internal dissipation is null, i.e. $\mathscr{P}_i(\mathbf{v}) = 0$. Therefore, the self-weight is the only source of strength that balances the external load.

3. Limit analysis theorems

Let the force V acting on the footing be of unitary magnitude ($V = 1$). The main objective of limit analysis is to find the maximum force μ, μ being a strictly positive parameter, that can be supported by the underlying soil. Two classical theorems, first proposed by Drucker et al. (1952), allow us to evaluate this limit load.

The *upper bound* theorem states that the load (or the load multiplier), determined by equating the internal power dissipation to the power expended by the external loads in a kinematically admissible velocity field $\mathbf{v}^{ka}$, is not less than the actual collapse load. As a consequence of the upper bound theorem, the actual load multiplier we seek is the lowest load multiplier:

$$\mu = \inf_{\mathbf{v}\in\mathscr{V}_{ad}} \mu^k(\mathbf{v}) \tag{18}$$

where

$$\mu^k(\mathbf{v}) = -\frac{\gamma\langle v_y\rangle}{v_y^c} \tag{19}$$

The *lower bound* theorem states that the load, determined from a stress field that satisfies equilibrium within the domain and on its boundary, and does not violate the yield condition, are not greater than the actual collapse load. Accordingly, the limit load is obtained as the supremum:

$$\mu = \sup_{\boldsymbol{\sigma}\in\mathscr{S}_{ad}} \mu^s(\boldsymbol{\sigma}) \tag{20}$$

The actual limit load is bracketed by the two load multipliers:

$$\mu^s \leqslant \mu \leqslant \mu^k \tag{21}$$

The limit theorems are most powerful when both types of solution can be computed so that the actual collapse load can be bracketed from above and below. This type of calculation provides a built-in error check on the accuracy of the estimated collapse load and is invaluable when an approximate solution is hard to obtain by other methods. Practical application of these theorems usually requires a numerical method, since analytical solutions are available only for a few problems involving simple geometries and basic loading conditions. However, care has to be taken to keep the bounding properties during the numerical treatment of these theorems. The most flexible numerical method is probably finite elements, since it allows us to consider problems with complex geometries, non-homogenous material properties, anisotropy and various loading conditions at the same time. UPPER and LOWER, developed by the Geotechnical Research Group at the University of Newcastle, are two such finite element limit analysis codes.

4. Numerical limit analysis

Soon after the fundamental theorems of limit analysis were established, linear programming techniques where implemented to determine the ultimate load capacity of discrete structures such as frames. It was subsequently realized that the use of the bound theorems could be extended to continua by combining them with the finite element method and mathematical programming techniques. The resulting methods, which we term finite element bound techniques, inherit all the benefits of the finite element approach and are applicable to a wide range of problems involving arbitrary domain geometries, complex loadings and heterogenous material properties. The discrete limit analysis theorems define non-linear convex mathematical programs. In early formulations, the non-linear problems were replaced by consistent linear ones (involving internal and external approximations of the Mohr–Coulomb criterion) that ensure the bounds are kept. The linear versions developed by Sloan (1988, 1989) have been used by Ukritchon et al. (2003) to derive bounds on the N_γ factor. Recently, more efficient non-linear programming schemes have been successfully implemented. These new techniques, employed here, allow much finer two-dimensional finite element meshes to be used, thus improving the quality of the bounds significantly. This paper updates the study described in Ukritchon et al. (2003) to give more accurate bounds on the N_γ factor. With these sharper bounds, the conclusions drawn in Ukritchon et al. (2003) are updated. We also suggest a semi-empirical formula that approximates the numerical results accurately.

4.1. Discrete formulation of the lower bound theorem

In the lower bound formulation, the stress field is discretized using finite elements with stress nodal variables according to

$$\boldsymbol{\sigma}(\boldsymbol{x}) = N_i(\boldsymbol{x})\boldsymbol{\sigma}_i \tag{22}$$

where $\boldsymbol{\sigma}_i$ is a nodal stress vector and $N_i(\mathbf{x})$ is a linear shape function. The shape function must be linear (Fig. 2a) to ensure that the yield criterion is satisfied everywhere if we enforce it only at the element nodes.

Linear equality constraints on the nodal stresses arise from the application of the equilibrium equations (2) and (3) over each element. By differentiating (22) and substituting into (2) and (3), the following linear equality constraints are obtained

$$\mathbf{A}^v\boldsymbol{\Sigma} = \mathbf{b}^v \tag{23}$$

where $\boldsymbol{\Sigma}$ is a global vector of nodal stresses, $\mathbf{A}^v$ is a matrix of equality constraint coefficients, and $\mathbf{b}^v$ is a vector of coefficients related to the body forces. Statically admissible stress discontinuities are permitted between each element in the domain by enforcing the equilibrium of the surface tractions acting on the sides of adjacent triangles. Since the shape functions are linear, the equilibrium condition is met by forcing all pairs of nodes on opposite sides of the discontinuity to have equal shear and normal stresses (Fig. 2b). By introducing standard transformation relations, these conditions take the following form

$$\mathbf{A}^{ed}\boldsymbol{\Sigma} = \mathbf{0} \tag{24}$$

The equilibrium conditions on the boundary (4), (5) or (6) and (7) generate extra linear equalities

$$\mathbf{A}^b\boldsymbol{\Sigma} = \mathbf{b}^b \tag{25}$$

where $\mathbf{A}^b$ is a matrix of equality constraint coefficients and $\mathbf{b}^b$ is a vector of coefficients related to the boundary loads. The previous equality constraints (23)–(25) may be assembled to give

$$\mathbf{A}, \boldsymbol{\Sigma} = \mathbf{b} \tag{26}$$

Unlike the more familiar displacement finite element method, where elements are connected at nodes, the nodal stresses are associated with a single element only (Fig. 2a). This follows from the fact that equilibrium requirements generate edge-to-edge conditions on the nodal unknowns, while compatibility relations are satisfied by a node-to-node condition (i.e. the condition that adjacent elements share the same nodal unknowns). The presence of statically admissible stress discontinuities between adjacent elements greatly improves the accuracy of the lower bound solution as they permit the stress field to change rapidly where

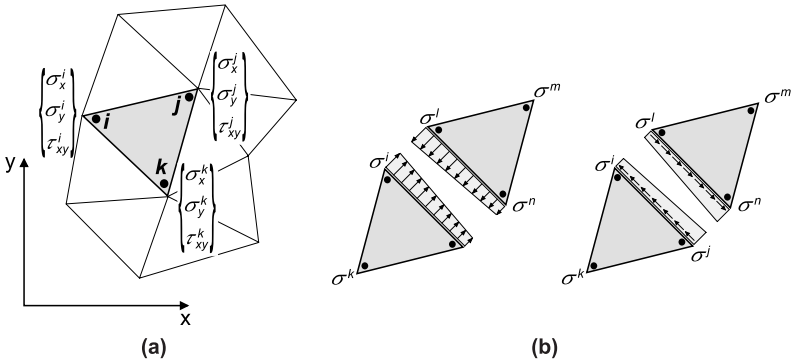

Fig. 2. (a) Linear stress element for lower bound. (b) Equilibrium of stress vector along stress discontinuity.

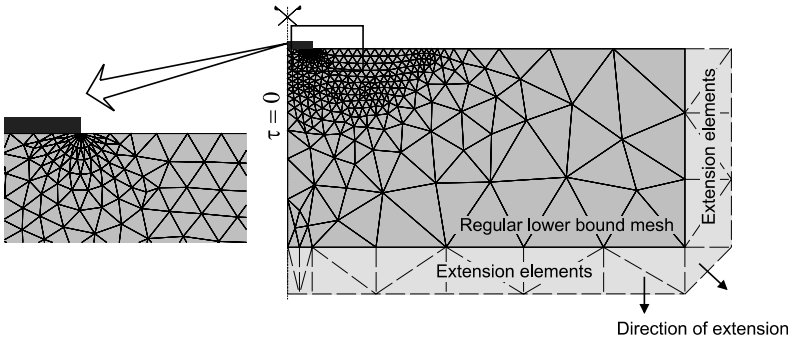

Fig. 3. Mesh refinement and extension elements for lower bound calculation.

needed. Special "extension" elements (Fig. 3) are also placed on a part of the boundary to model an unbounded domain, thus providing a complete statically admissible stress field and a rigorous lower bound. To enhance the accuracy of the lower bound, a refined mesh is used in the vicinity of the footing with a dense fan of discontinuities at the singularities centered on the singularity at the edges of the footing (Fig. 3).

The discretized version of the lower bound theorem takes the form of a non-linear constrained optimization problem. The objective function of this non-linear programming problem, which corresponds to the collapse load, is maximized according to

$$\begin{aligned} &\max_{\boldsymbol{\Sigma}} && \mathbf{C}^{\mathrm{T}}\boldsymbol{\Sigma} \\ &\text{subject to} && \begin{cases} \mathbf{A}\boldsymbol{\Sigma} = \mathbf{b} \\ f_i(\boldsymbol{\sigma}) \leqslant 0 \quad i = \{1,\ldots,n\} \end{cases} \end{aligned} \tag{27}$$

where $\mathbf{C}$ is a vector of objective function coefficients which defines the collapse load $\mathbf{C}^{\mathrm{T}}\boldsymbol{\Sigma}$, f_i, $(\boldsymbol{\sigma})$ is the yield function for node i, and n is the number of nodes. In earlier formulations, non-linear constraints on the nodal stresses, arising from the satisfaction of the yield criterion, were avoided by linearizing the yield surface. Although this strategy proved successful for the solution of two-dimensional stability problems, it is unsuitable for three-dimensional geometries since a huge number of inequalities will inevitably be generated. The present approach uses the yield criterion in its native non-linear form and is well suited for any convex yield surface. Full details of the formulation, along with references to earlier works, can be found in Lyamin and Sloan (2002b). The solution to the mathematical problem (24), which constitutes a statically admissible stress field, can be obtained efficiently by solving the system of non-linear equations that define its Kuhn-Tucker optimality conditions. The two-stage quasi-Newton solver used for this purpose usually requires less than about 50 iterations, regardless of the problem size, and the resulting algorithm is many times faster than an equivalent linear programming one (Lyamin and Sloan, 2002b).

4.2. Discrete formulation of the upper bound theorem

The minimum principle (15) is cast in discrete form by expressing the velocity field as function of a finite number of parameters. Plane finite elements based on velocity approximations are employed for this purpose. In each element $E(E = 1,\ldots,N)$ the velocities are expressed as

$$\mathbf{v}(\boldsymbol{x}) = N_i(\boldsymbol{x})\mathbf{v}_i \tag{28}$$

where $\mathbf{v}_i$ is a nodal velocity vector and $N_i(\boldsymbol{x})$ is the shape function. The linear three-noded triangle (Fig. 4a) is used to model the velocity field. This choice of element ensures that the upper bound is strict since, with a

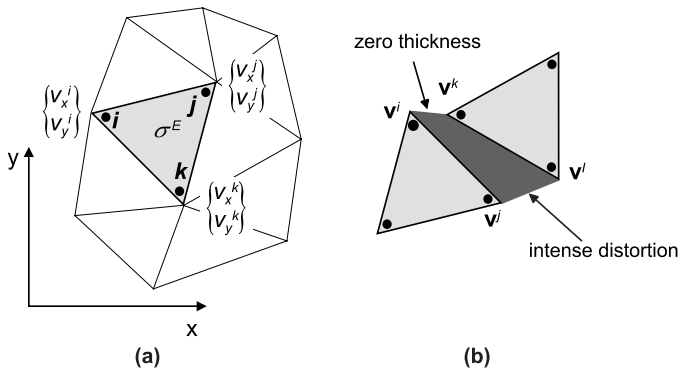

Fig. 4. (a) Linear velocity finite element for upper bound. (b) Kinematically admissible velocity discontinuity.

constant plastic strain rate, the flow rule is satisfied everywhere. Two unknown velocities are associated with each node, and a single plastic multiplier rate, plus a constant stress vector, are associated with each element. To improve the upper bound calculations and avoid the well-known phenomenon of locking that may occur for incompressible materials, Sloan and Kleeman (1995) proposed a formulation that allows kinematically admissible velocity discontinuities (Fig. 4b) along all shared element edges in the mesh. In their procedure, the direction of shearing is chosen automatically during the minimization process to give the least amount of dissipated power. This formulation is computationally efficient and gives good estimates of the true limit load with a relatively coarse mesh. To avoid the Kuhn-Tucker constraints, the minimum problem can be transformed into a min-max problem. As a result of this transformation, the plastic multiplier rate does not appear explicitly in the formulation, thus reducing the size of the problem. Once the constraints and the objective function coefficients are assembled, the task of finding a kinematically admissible velocity field, which minimizes the internal power dissipation for a specified set of boundary conditions, may be written as

$$\max_{\boldsymbol{\Sigma}} \min_{\mathbf{V},\mathbf{D}} \quad \boldsymbol{\Sigma}^{\mathrm{T}}\mathbf{B}\mathbf{V} + \mathbf{C}_u^{\mathrm{T}}\mathbf{V} + \mathbf{C}_d^{\mathrm{T}}\mathbf{D}$$
$$\text{subject to} \quad \begin{cases} \mathbf{A}_u\mathbf{V} + \mathbf{A}_d\mathbf{D} = \mathbf{b} \\ f_i(\boldsymbol{\sigma}) \leqslant 0 \quad E = \{1, \ldots, N\} \\ \mathbf{D} \geqslant \mathbf{0} \end{cases} \tag{29}$$

where $\mathbf{V}$ is a global vector of unknown velocities, $\mathbf{D}$ is a global vector of unknown discontinuity variables, $\boldsymbol{\Sigma}$ is a global vector of unknown element stresses, $\mathbf{C}_u$ and $\mathbf{C}_d$ are vectors of objective function coefficients for the nodal velocities and discontinuity variables, $\mathbf{A}_u$ and $\mathbf{A}_d$ are matrices of equality constraint coefficients for the nodal velocities and discontinuity variables, $\mathbf{B}$ is a global matrix of compatibility coefficients that operate on the nodal velocities, $\mathbf{b}$ is a vector of coefficients, f_i, $(\boldsymbol{\sigma})$ is the yield function for element i, and N is the number of triangular elements. The objective function $\boldsymbol{\Sigma}^{\mathrm{T}}\mathbf{B}\mathbf{V} + \mathbf{C}_u^{\mathrm{T}}\mathbf{V} + \mathbf{C}_d^{\mathrm{T}}\mathbf{D}$ corresponds to the total dissipated power, with the first term giving the dissipation in the continuum, the second term giving the dissipation due to fixed boundary tractions or body forces, and the third term giving the dissipation in the discontinuities. Note that the size of the discretized domain must be large enough to contain all potential failure surfaces, with the far field boundaries being subjected to a zero velocity condition (Fig. 5). As expected, mesh refinement at the footing edges improve the accuracy of the solution (Fig. 5).

The solution to the optimization problem (26), which defines a kinematically admissible velocity field, can be computed efficiently using a variant of the scheme developed for the non-linear lower bound method (Lyamin and Sloan, 2002a).

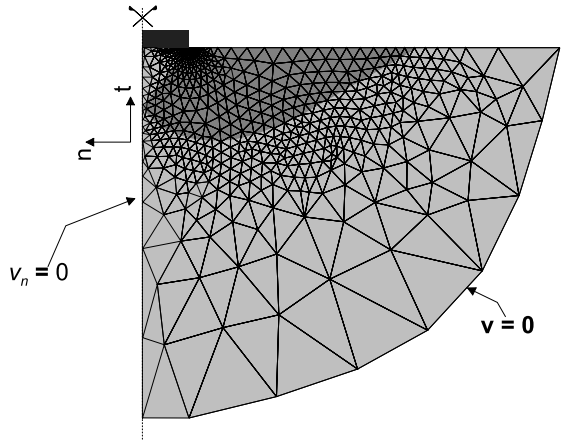

Fig. 5. Mesh refinement and boundary conditions for upper bound calculation.

The discrete formulations of the limit analysis theorems described above are used here to estimate the bearing capacity of a surface footing resting on a cohesionless soil with self-weight. The rigorous ultimate load is computed with an error that does not exceed 3.42%. Before presenting the results of our study, we review previous contributions on the bearing capacity factor N_γ.

5. Estimations of N_γ–previous work

In this section, we summarize previous studies on the bearing capacity factor N_γ that have been published. The results are presented according to the method used, which is briefly recalled.

5.1. The limit equilibrium method

The bearing capacity of shallow footings is a topic with a long history. The basic structure of the bearing capacity formula has not changed since the fundamental work of Terzaghi (1943), who suggested the simple analytical bearing capacity equation (1). Terzaghi used the limit equilibrium method to calculate the bearing capacity factors. In this technique, collapse is assumed to occur as a result of sliding on a rupture surface and the failure criterion is assumed to be satisfied within the soil mass. The shape of the failure mechanism, composed of simple geometrical entities, is chosen on physical grounds. Equilibrium is enforced at the global level by considering each part of the mechanism as a free body subjected to forces, some of which are related to the strength properties of the soil. In this sense, the method is purely static. Nothing is said about the stress distribution anywhere except on the rupture surface. To remove any static indeterminacy that may occur, assumptions are made regarding the force distributions. A systematic search is then performed to find the particular surface for which the computed collapse load is the lowest. For his calculations, Terzaghi assumed a Prandtl-type failure surface (Fig. 6), which is composed of a rigid active wedge, a radial shear zone, and a rigid passive wedge. The radial shear zone is bounded by a log-spiral curve. Since the stress field is not defined, it is not known whether the solution is a lower bound. Provided the form of the rupture surface is chosen with reasonable care, the error in the computed collapse load should be small. If, however, the assumed surface differs greatly from the true one, the error may be considerable. It will be shown in this paper that the failure surface differs significantly from the Prandtl one when self-weight is taken into account. For a weightless soil, the log-spiral is unique and centered at the footing edge. It spans

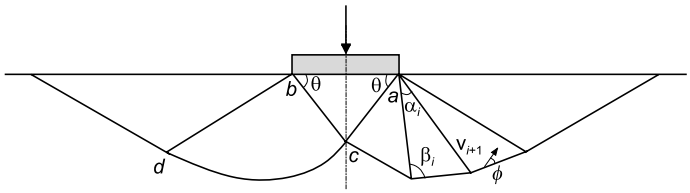

Fig. 6. Prandtl mechanism: continuous and rigid-block collapse pattern.

between bc and bd, which, respectively, make angles of ϕ and $\frac{\pi}{2}-\phi$ with the horizontal. Closed form expressions for N_c and N_q may be obtained by using moment equilibrium equations. For a weightless soil, the critical surface is the Prandtl one (Fig. 6) and the method gives exact solutions for N_c and N_q:

$$N_q = \mathrm{e}^{\pi\tan\phi}\tan^2\left(\frac{\pi}{4}+\frac{\phi}{2}\right), \quad N_c = (N_q-1)\cot\phi \tag{30}$$

This type of log-spiral is unsatisfactory for calculating N_γ. Terzaghi therefore assumed that the center of the log-spiral lies on bd (Fig. 6) and found the most critical one using a graphical method. More than three decades later Kumbhojkar (1993) used a similar approach, but derived an analytical expression for N_γ and compared his estimates with those of Terzaghi. He found large differences for high friction angles and attributed this discrepancy to the approximate nature of the graphical method used by Terzaghi. In 1951, Meyerhof (1951) published a bearing capacity theory which could be applied to both shallow and deep foundations. His theory is based on the limit equilibrium method but uses a slightly different failure surface to take into account the shear strength of the overlying soil. The radial shearing zone is still defined by a log-spiral which is optimized using a semi-graphical method. A few years later, Meyerhof (1963) provided an analytical expression for N_γ that approximates the results obtained with the semi-graphical method. He suggested an expression for the N_γ factor that is very similar to the N_c factor, i.e.:

$$N_\gamma = (N_q-1)\cot(1.4\phi) \tag{31}$$

Using a limit equilibrium approach, Zhu et al. (2001) adopted a Prandtl-type mechanism and employed the method of slices to calculate the passive earth pressure. Three values of the angle θ (see Fig. 6) were considered: (a) $\theta=\phi$, (b) $\theta=\frac{\pi}{2}+\frac{\phi}{2}$ and (c) θ such that N_γ is a minimum.

5.2. Slip-line method

A more mathematically rigorous approach for stability analysis of geotechnical structures is the slip-line method. Several investigators including Sokolovskii (1965), Lundgren and Mortensen (1953), Hansen (1970), Booker (1969), Bolton and Lau (1993) and Kumar (2003) have applied this method to estimate bearing capacity factors. In the slip-line technique, the Coulomb yield criterion is combined with the equations of equilibrium to give a set of differential equations of plastic equilibrium which, together with the stress boundary conditions, can be used to investigate the stresses in the soil beneath a footing at the point of incipient failure. The solution proceeds by constructing two intersecting families of curvilinear slip-lines (α-lines and β-lines) from known stresses at the boundary. For a rigorous lower bound, it must also be shown that, in the rigid regions surrounding the zones of plastic equilibrium, a statically admissible state of stress exists. The solutions obtained from this method are generally not exact collapse loads, since it is not always possible to integrate the stress-strain rate relations to obtain a kinematically admissible field or to extend the stress field over the entire half-space of the soil domain. Furthermore, the method can only deal with problems in which the boundary conditions are stated in terms of surface tractions, so the problem is statically determinate. Therefore, if there are restrictions on the boundary displacements (as in the

case, for example, of a rigid foundation with a rough or smooth interface), assumptions need to be made about the distribution of stress on the boundary before a solution is possible. The solution may prove to be very sensitive to these assumptions, particularly if the self-weight is taken into account.

There are very few closed form solutions to the slip-line equations, but many approximate answers have been obtained. A widely used procedure is the approximate finite difference scheme suggested by Sokolovskii (1965). For ponderable soils, Sokolvskii concludes that at least one family of the slip-lines must be curved (Fig. 7). Since Sokolvskii's numerical scheme always requires a small surcharge q, it cannot completely isolate the effect of the soil weight γ. A novel slip-line solution for bearing capacity problems with self-weight was proposed by Lundgren and Mortensen (1953). They considered a failure mechanism where the trapped wedge is bounded by curved slip lines that are tangential to the footing edges and terminate along the center line of the foundation with an interior angle equal to $\frac{\pi}{2} - \phi$. Within the radial shearing zone, the slip lines (α-lines and β-lines) are both curved but become straight in the passive shearing zone (Fig. 7). Lundgren and Mortensen solved the problem numerically by applying the Kármán (1926) postulate in order to avoid numerical difficulties that arise when no surcharge is considered. They computed the value of N_γ only for $\phi = 30°$. Their result of $N_\gamma = 14.8$ corresponds to 70% of the value generally applied. The Lundgren and Mortensen solution is incomplete, since it contains no discussion of the velocity field and does not show that the stress field can be extended into the rigid region without violating the yield criterion. The same slip-line network was later considered by Larkin (1968) for circular footings. Hansen and Christensen (1969) also used the same rupture figure and provided numerical values of N_γ in charts. Later, Hansen (1970) suggested the following semi-empirical expression that approximates the numerical results obtained by the slip-line method:

$$N_\gamma = 1.5(N_q - 1)\tan\phi \tag{32}$$

Vesić (1975) suggested, a few years later, a slightly modified formula

$$N_\gamma = 2(N_q - 1)\tan\phi \tag{33}$$

This expression is a closed-form approximation of an earlier slip-line solution by Caquot and Kérisel (1953). Booker (1969) used the slip-line method and provided numerical values of N_γ in charts. For the smooth footing he was able to derive a velocity field associated with the stress field. Since the stress field was not extended into the rigid region, this result provides only an upper bound on N_γ. Later, Poulos et al. (2001) suggested the following expressions that approximate the numerical results obtained by Booker:

$$\text{rough: } N_\gamma \simeq 0.1045\mathrm{e}^{9.6\phi}, \quad \text{smooth: } N_\gamma \simeq 0.0663\mathrm{e}^{9.3\phi} \tag{34}$$

where ϕ is given in radians and $N_\gamma = 0$ if $\phi = 0$. Bolton and Lau (1993) used the method of characteristics to estimate the vertical bearing capacity of circular and strip footings resting on ponderable soils. For smooth footings, they used a shallow Hill mechanism while for rough footings they adopted a deep Prandtl mechanism with a triangular wedge. Recently, Kumar (2003) proposed another slip-line solution based on Lundgren and Mortensen's failure mechanism. He used the standard finite difference procedure of Sokolovskii.

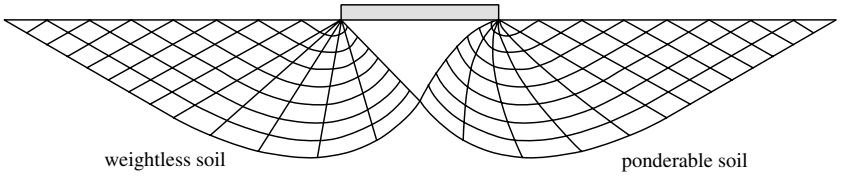

Fig. 7. Slip-lines: weightless and ponderable soil.

All calculations were performed first using the forward difference scheme, with the accuracy of the computations being subsequently increased by using a central difference scheme. The net of stress characteristics used was dense and, to avoid numerical problems, a small surcharge was always imposed.

5.3. Upper bound method

In the rigid-block upper bound method, a mechanism composed of triangular rigid blocks that move with constant velocities is considered (see Fig. 6). The wedge *abc* is assumed to move vertically as a rigid body with the same initial downward velocity as the footing $\mathbf{v}^c$. The downward movement of the wedge *abc* is accommodated by the lateral movement of adjacent soil. The variables are the independent angles θ, α_i, and β_i, which give some flexibility in choosing the most critical mechanism. Since no continuous plastic deformation of the soil mass is permitted to occur, the power is dissipated solely at the interfaces between adjacent blocks, which constitute velocity discontinuities, and between blocks in motion and soil at rest. Kinematical admissibility requires that the velocity jump must be inclined at an angle of ϕ to the discontinuity surfaces. Under the assumption of an associated flow rule, it can be proved that the dissipation is a function only of the velocities. This property is used to compute the dissipation along the discontinuities where the magnitudes of the velocity jumps have been determined from geometrical relations in the velocity diagram. The geometry is optimized to yield the minimum dissipated power and, hence, the corresponding collapse load. During the last decade, this approach has been encouraged by the work of Drescher and Detournay (1993), who treated non-associated flow by using modified strength properties. Various studies with the rigid-block technique use different mechanisms and solution methods to obtain the lowest upper bound. For a rough footing, Michałowski (1997) considered a Prandtl-like mechanism where the shear zone is composed of *n* triangular rigid-blocks. He performed calculations using two schemes: (a) a scheme where the minimum sum is sought and the three bearing capacity factors are consistent with one mechanism, and (b) an ''all-minimum'' scheme where each term of Eq. (1) is minimized with (possibly) different mechanisms to give a conservative estimate for q_u. In the latter scheme, N_γ becomes a function of ϕ only, but the geometry of the mechanism for which N_γ reaches its minimum is no longer consistent with that for N_c and N_q. We will use these results for comparison. For smooth footings, Michałowski (1997) concluded that the rigid-block mechanism of Hill gives better results.

Soubra (1998) used a similar method and provided results that are almost identical to those obtained by Michałowski. In a subsequent paper, Wang et al. (2001) suggested the use of a quadrilateral block in the radial shearing zone of a Prandtl-like mechanism. They compared results with and without the simultaneous influence of the cohesion, the surcharge and the self-weight, and found that the bearing capacity factors are slightly higher when all factors are taken into account at the same time. Their numerical values for the individual bearing capacity factors are higher than those obtained by Michałowski (1997). Zhu (2000) proposed a faster method to determine the critical failure surface and hence the bearing capacity factor N_γ. The technique is based on an equivalence between the limit equilibrium and rigid-block mechanism methods. The results obtained are identical to those of Michałowski (1997).

5.4. Finite elements simulations

The displacement finite element technique can also be used to derive approximate estimates of the bearing capacity factors. In the study of Griffiths (1982), the soil was represented by an elasto-plastic model with a Mohr–Coulomb yield condition, in conjunction with a non-associated flow rule (no plastic volume change). The soil mass was modeled by a relatively coarse mesh composed of 8-noded quadrilateral isoparametric elements with 2×2 reduced quadrature. The solution algorithm adopted was the viscoplastic initial strain method of Zienkiewicz (1974) with a simple forward Eulerian integration in time. Due to numerical convergence problems, Griffiths (1982) did not investigate cases where the friction angles exceed 35°. To

isolate the N_γ term in Eq. (1), a cohesionless ponderable soil with no surface surcharge was considered. The self-weight of the soil was taken into account by attributing an initial stress state at all the quadrature points. The vertical stress was taken as the product of γ and the depth of the integration point from the ground surface, while the horizontal stress was set to the vertical stress multiplied by the coefficient of earth pressure at rest K_0. Analyses were carried out by applying incremental downward velocities to the surface nodes below the footing. Rough and smooth footing interfaces were simulated, respectively, by fixing or freeing the lateral movement of nodes in contact with the footing. A surprising conclusion of the study is a slight dependance of N_γ on the footing width. This effect was later recognized as being due to the mesh arrangement (Woodward and Griffiths, 1998) and the method used to compute N_γ (where the vertical stress at the Gauss points was employed to determine the bearing capacity). A more consistent approach, as pointed out by Day and Potts (2000), is to sum the nodal reaction forces to obtain the equivalent footing load. As expected, the stress singularity at the edge of the footing influences the computed bearing capacity considerably and can give the illusion that N_γ is size-dependent. An extension of Griffith's work to circular footings was carried out by Manoharan and Dasgupta (1995).

The effect of friction angles on the bearing capacity were considered by Frydman and Burd (1997). Their work used two different numerical techniques to estimate N_γ; namely, the finite-difference and finite element methods. Most of their solutions were obtained using a finite-difference program (FLAC), with the remainder being found from a finite element code developed at the university of Oxford (OXFEM). Their finite element calculations used unstructured meshes of six-noded isoparametric triangles with three Gauss points. In the vicinity of the footing, a relatively dense mesh pattern was adopted. The elastoplastic soil model employed the Matsuoka yield function, with its material parameters being selected so it corresponded to the Mohr–Coulomb model under plane strain loading. They used a tangent stiffness approach to solve the finite element algebraic equations, but little is said on how the self-weight was taken into account.

All the finite element calculations discussed above constitute, at best, a pseudo-upper bound to the exact solution. This is because a rigorous upper bound solution requires the flow rule to be satisfied everywhere and not only at the Gauss points. This suggests the use of linear finite elements, but these suffer from locking unless special quadrature schemes are adopted (Nagtegaal et al., 1974). Moreover, the use of an explicit stress integration scheme does not ensure that the flow rule is satisfied at the end of each time step.

6. Results and discussion

The present study of the bearing capacity factor N_γ is conducted for smooth and rough footings on soil with friction angles ϕ ranging from 5° to 45°. Since N_γ is independent of B, the calculations can be carried out for a generic footing width. In the following, N_γ was calculated using Terzaghi's expression

$$N_\gamma = \frac{V_{ult}}{0.5B^2\gamma}$$

where V_{ult} is the total ultimate load. To achieve tight bounds, very fine meshes have been used which depend on the value of the friction angle ϕ. The lower bound computations have been carried out on half of the domain using 4346 elements and 6324 discontinuities. These number were kept constant regardless of ϕ or the nature of the soil-footing interface. Only the size of the meshed domain was increased with an increasing value of ϕ so that the meshed domain contained the plastic zone. On the centerline, the symmetry condition imposes a null shear traction distribution (see Fig. 3). For the upper bound calculations, we again take advantage of the symmetric nature of the problem and model only one-half of the domain. To ensure tight bounds, the number of elements and discontinuities in the upper bound meshes need to be increased with increasing ϕ. Table 1 gives the essential characteristics of the meshes used in the upper bound calculations for all friction angles and footing roughness conditions. The numerical results are presented in

Table 1
Upper bound mesh characteristics

ϕ (°)	Rough footing		Smooth footing	
	Elements	Discontinuities	Elements	Discontinuities
5	3850	5730	3927	5845
10	3850	5730	8775	13095
15	4590	6836	15700	23460
20	4590	6836	15700	23460
25	4590	6836	15700	23460
30	5650	8415	15700	23460
35	5410	8057	15700	23460
40	12735	19013	15700	23460
45	12735	19013	20815	31119

Table 2
Bounds for N_γ–rough and smooth footing

ϕ (°)	Rough footing			Smooth footing		
	N_γ^{LB}	N_γ^{UB}	± Error (%)	N_γ^{LB}	N_γ^{UB}	± Error (%)
5	0.1154	0.1196	1.79	0.0862	0.0914	2.93
10	0.4338	0.4552	2.41	0.2827	0.2993	2.85
15	1.1780	1.2378	2.48	0.7005	0.7370	2.54
20	2.8219	2.9612	2.41	1.5780	1.6650	2.68
25	6.4313	6.7379	2.33	3.4538	3.6534	2.81
30	14.5671	15.2372	2.25	7.6225	8.0784	2.90
35	33.9506	35.6491	2.44	17.4645	18.5134	2.92
40	83.3268	88.3901	2.95	42.7699	45.4236	3.01
45	224.9452	240.8801	3.42	115.6237	123.2515	3.19

Table 2. For practical purposes N_γ needs to be estimated only to one decimal point. To compare our results with other solutions, however, all results in tables are truncated to four digits. As expected, the bearing capacity factor N_γ increases rapidly with increasing ϕ (Table 2). As it can be seen from this Table, the bounds for the rough and smooth cases are very tight, and the maximum error, defined as

$$\text{Error} = \frac{N_\gamma^{UB} - N_\gamma^{LB}}{N_\gamma^{UB} + N_\gamma^{LB}} \times 100 \tag{35}$$

is at most equal to 3.42%. With such a small gap between the lower and upper bounds, their average can be considered to be very close to the exact value of N_γ. Indeed, the maximum difference between the exact solution and the average of the lower and upper bounds, N_γ^{AV}, is at most ±3.42%. The accuracy of the results obtained stems from the solution algorithm adopted. For a frictional material, using the yield function in its native form removes the linearization error that is present in linear programming formulations. Moreover, quasi-Newton non-linear programming solvers have proven particularly efficient in solving large scale limit analysis problems, thus allowing very fine meshes to be used. The numerical results for the rough footing can be accurately approximated by the function

$$N_\gamma = e^{\frac{1}{6}(\pi + 3\pi^2 \tan\phi)} \tan^{\frac{2\pi}{5}} \phi \tag{36}$$

This expression for the bearing capacity factor N_γ is applicable for the full range of internal friction angles considered and can be employed in design. If we compute N_γ using two decimals, the formula (36) furnishes estimates that are always within the numerical bounds. This implies that the proposed expression for N_γ will have a maximum error which is at most ±3.42%.

Table 3
Footing roughness factor β

ϕ	5°	10°	15°	20°	25°	30°	35°	40°	45°
β	0.76	0.65	0.60	0.56	0.54	0.53	0.52	0.51	0.51

As expected, the footing roughness has a significant influence on the bearing capacity factor N_γ. Table 3 shows the roughness factor β, defined as ratio of N_γ^{AV} for a smooth footing to N_γ^{AV} for a rough footing. This reduction coefficient can be approximated using the following equation

$$\beta = \sum_{i=0}^{5} a_i \tan^i \phi \tag{37}$$

where $a_0 = 0.9232$, $a_1 = -2.4101$, $a_2 = 6.4821$, $a_3 = -9.4059$, $a_4 = 6.991$ and $a_5 = -2.0675$. We observe that the reduction in the N_γ factor is around 50% for friction angles ranging from 20° to 45°. This is in good agreement with Meyerhof's suggestion that N_γ for a smooth footing is roughly half that for a rough footing.

Fig. 8 shows the plastic zones obtained from various upper bound calculations with friction angles equal to 45° (smooth and rough footing) and 30° (rough footing). As expected, the size of the plastic zone for a

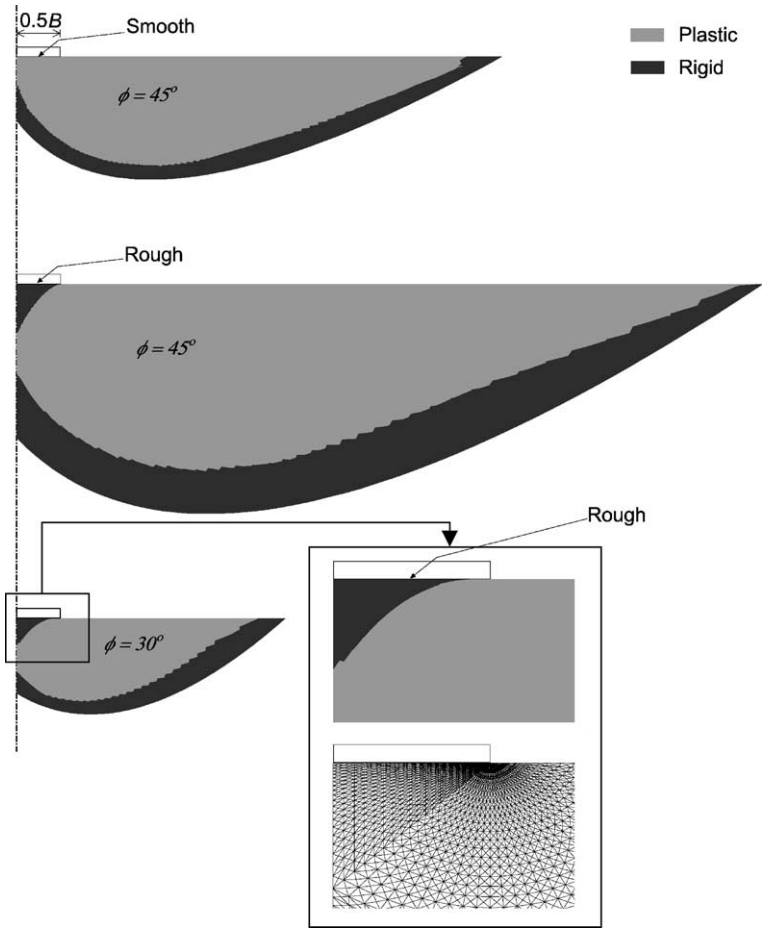

Fig. 8. Plastic zones from upper bound calculations.

smooth footing is smaller than that for an equivalent rough one. The extent and depth of the plastic zone increases as the friction angle increases. For the rough case, a curved rigid wedge immediately underneath the footing can be clearly seen. The boundary of this wedge appears to be tangent to the footing near its edge, as assumed by Lundgren and Mortensen (1953). Fig. 9 shows a plot of the plastic zone in the vicinity of the footing, as obtained from a lower bound calculation for $\phi = 45°$ and a rough soil-foundation interface. The shape of the rigid wedge is very similar to that for the upper-bound failure mechanism. If the soil-foundation interface is smooth, the soil just below the footing becomes plastic and there is no rigid wedge (Fig. 10). The appearance of the lower bound plastic zone suggests a Hill-type failure mechanism. We observe that edges of the failure mechanism are curved. Investigators using the rigid-block method have generally found that the Hill mechanism provides better results for the smooth footing case (Michałowski, 1997). The computed velocity field on the free surface next to the footing, for $\phi = 45°$, is shown in Fig. 11 for a rough interface and in Fig. 12 for a smooth interface.

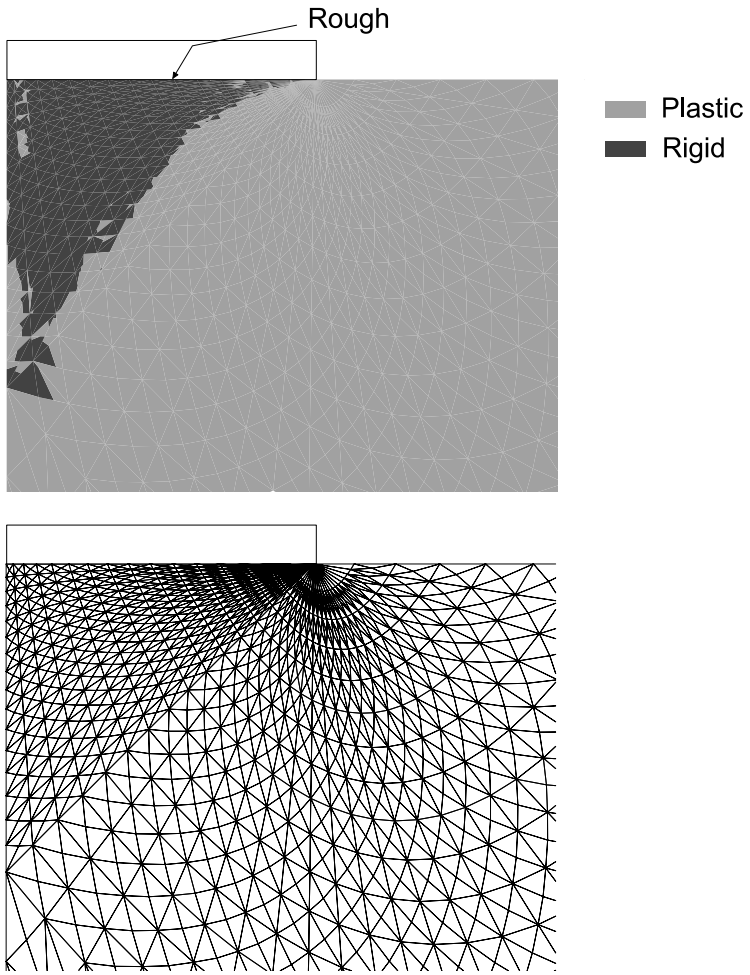

Fig. 9. Lower bound plastic zone in the vicinity of rough footing–$\phi = 45°$.

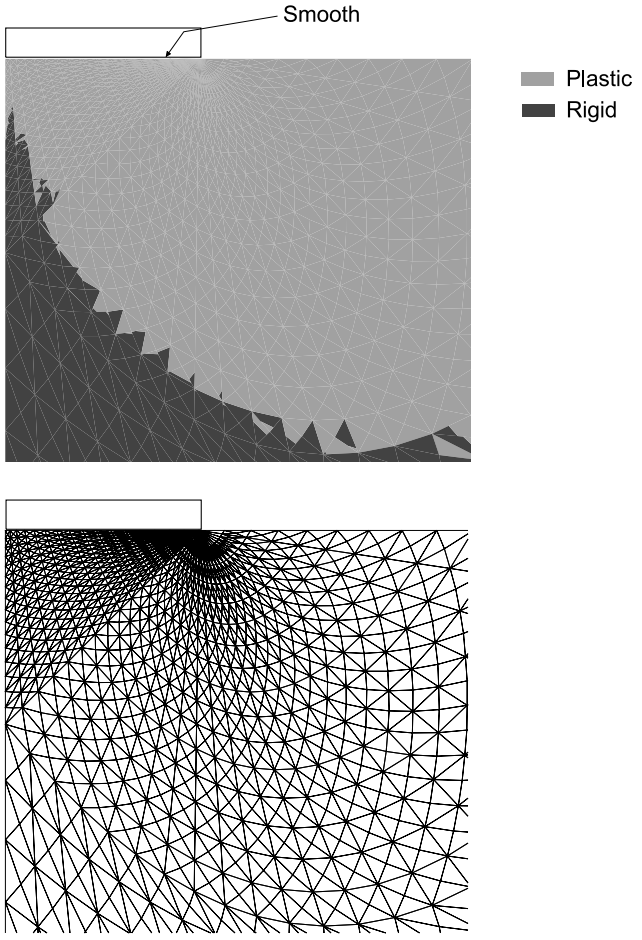

Fig. 10. Lower bound plastic zone in the vicinity of smooth footing–$\phi = 45°$.

These plots suggest that the velocity directions are very similar for the two cases. For a rough interface, the magnitude of the velocity next to the footing is higher than that for a smooth interface. This magnitude, however, decreases more rapidly as we move away from the footing edge.

The new numerical results are now compared with analytical expressions provided by Hansen (1970), Meyerhof (1963) and Vesić (1975) for a rough footing. These expressions are widely used in design standards and it is important to assess them. We also compare our results with other numerical results that have been reported in the literature. The computed value of N_γ^{AV}, the estimates of N_γ given by (36) and (37), and other selected solutions are presented in Tables 4 and 5 for rough and smooth footings, respectively.

A comparison between N_γ^{AV} and various selected solutions is shown on a semi-log plot in Fig. 13 for a rough footing and Fig. 14 for a smooth footing. For the latter case, Meyerhof has suggested the use of N_γ for a rough footing divided by 2. For $\phi \geqslant 10°$, $\log(N_\gamma^{AV})$ can be approximated as a linear function of the friction angle for both smooth and rough interfaces. For a rough footing, Vesić's formula gives N_γ estimates that are always unconservative. The difference between these values and N_γ^{AV} is particularly significant for $\phi \leqslant 20°$, but reduces with increasing friction angle. For a friction angle of 45°, Vesić formula overestimates the bearing capacity factor N_γ^{AV} by 17%, while for $\phi = 5°$ it overestimates it by 282%. For a rough footing, the Meyerhof method gives better results for low friction angles and is conservative for $\phi \leqslant 25°$. For higher

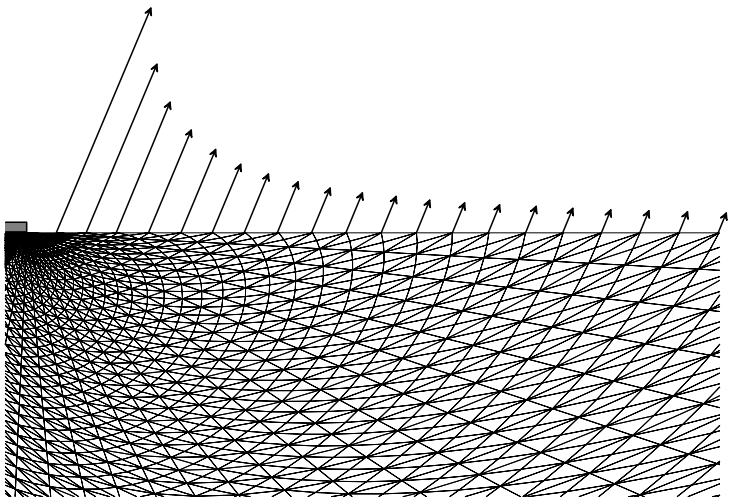

Fig. 11. Velocity field near rough footing–$\phi = 45°$.

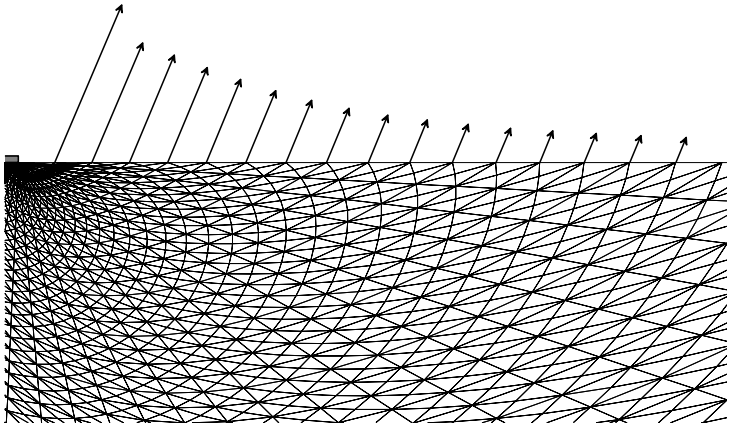

Fig. 12. Velocity field near smooth footing–$\phi = 45°$.

Table 4
Comparison of N_γ values for rough footing

ϕ (°)	N_γ^{AV}	N_γ (Eq. (36))	Booker (Eq. $(34)_1$)	Hansen	Meyerhof	Vesić	Michalowski	Bolton and Lau	Frydman and Burd	Kumar	Zhu et al.
5	0.117	0.122	0.244	0.075	0.070	0.449	0.181	0.620	–	0.23	0.107
10	0.445	0.455	0.563	0.389	0.367	1.224	0.706	1.710	–	0.69	0.453
15	1.208	1.210	1.301	1.182	1.129	2.648	1.938	3.170	–	1.6	1.309
20	2.892	2.857	3.007	2.948	2.871	5.386	4.468	5.970	–	3.43	3.367
25	6.585	6.463	6.950	6.758	6.766	10.876	9.765	11.6	–	7.18	7.864
30	14.902	14.621	16.064	15.070	15.668	22.402	21.394	23.6	21.7	15.57	17.579
35	34.800	34.163	37.126	33.921	37.152	48.029	48.681	51	54.2	35.16	40.2
40	85.858	85.110	85.805	79.541	93.691	109.411	118.827	121	147	85.73	97.926
45	232.913	234.722	198.310	200.811	262.742	271.748	322.835	324	422	232.84	263.746

Table 5
Comparison of N_γ values for smooth footing

ϕ (°)	N_γ^{AV}	N_γ (Eqs. (36) and (37))	Booker (Eq. $(34)_2$)	Meyerhof	Bolton et al.	Michalowski
5	0.0888	0.092	0.149	0.035	0.09	0.127
10	0.2910	0.298	0.336	0.183	0.29	0.423
15	0.7187	0.720	0.757	0.565	0.71	1.050
20	1.6215	1.602	1.704	1.435	1.6	2.332
25	3.5536	3.490	3.836	3.383	3.51	5.02
30	7.8504	7.696	8.636	7.834	7.74	10.918
35	17.9890	17.668	19.443	18.576	17.8	24.749
40	44.0967	43.707	43.775	46.845	44	60.215
45	119.4376	120.365	98.557	131.371	120	164.308

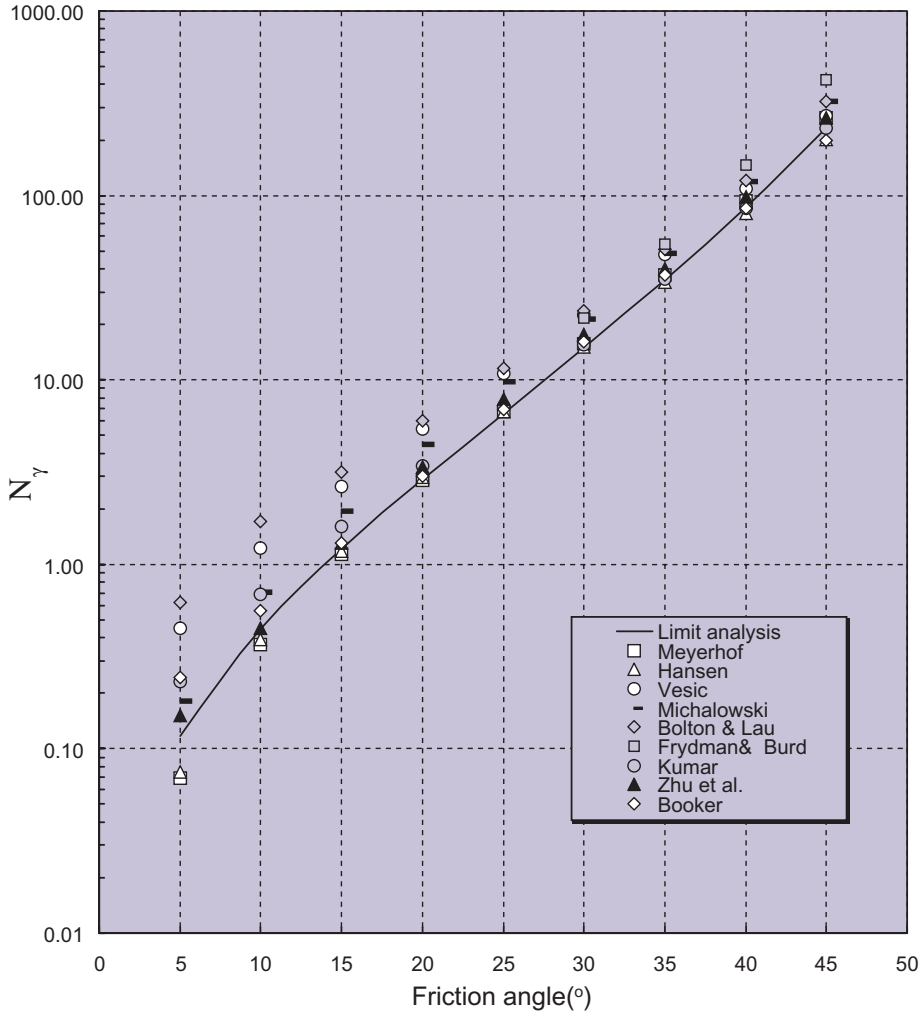

Fig. 13. Comparison of N_γ values for rough footing.

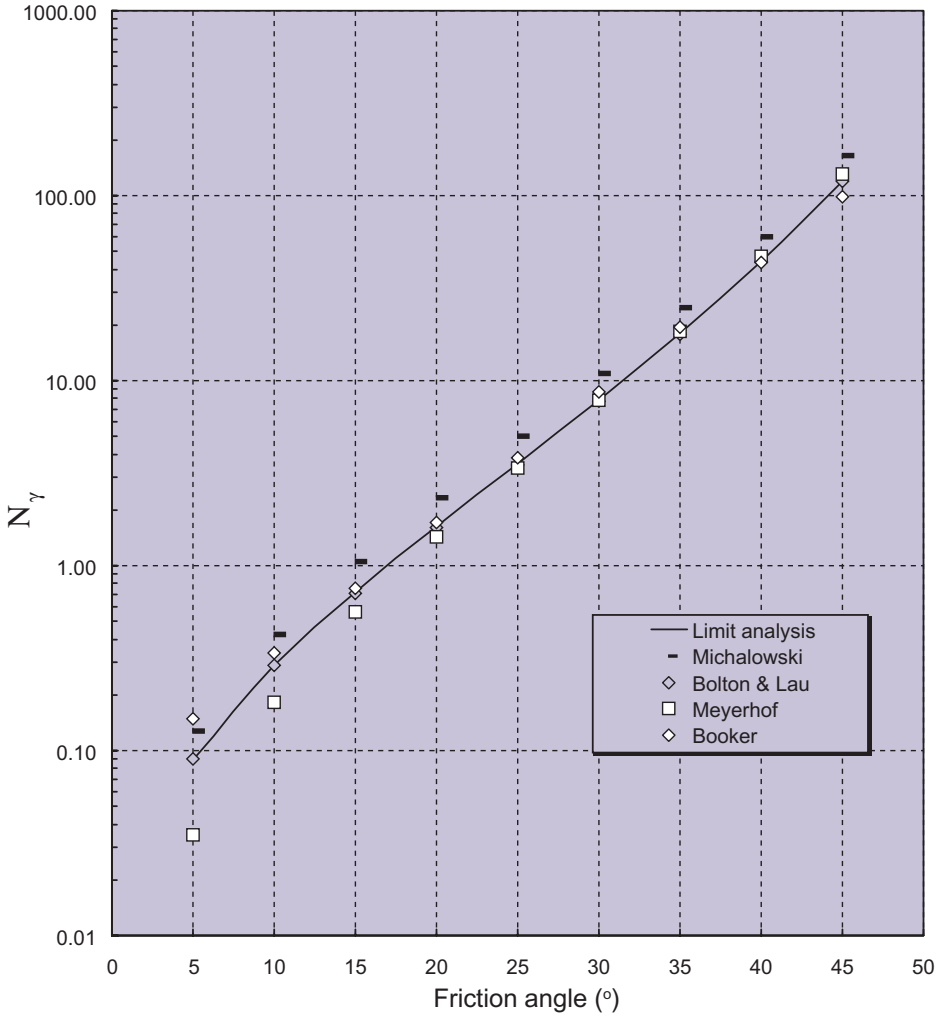

Fig. 14. Comparison of N_γ values for smooth footing.

friction angles, it overestimates N_γ^{AV} (by 13% for $\phi = 45°$). In contrast, the Hansen formula always underestimates the effect of the soil weight for a rough footing, with the largest difference from N_γ^{AV} occurring at very low friction angles (5°–10°). For typical frictional angles, ranging between 30° and 45°, the Hansen formula under estimates N_γ by 14% at most. The difference between the Hansen and Meyerhof solutions is a result of the failure mechanism assumed and the calculation method adopted. Meyerhof used a Prandtl-like mechanism, with a rigid wedge of triangular shape, whilst Hansen considered a similar mechanism but with a curved wedge. The analytical expression provided by Poulos et al. (2001) appears to be in good agreement with N_γ^{AV} for most values of the friction angle, except for very low/high friction angles where it overestimates/underestimates N_γ^{AV}. The results obtained for a rough footing by Michałowski, using the ''all-minimum'' scheme, are significantly higher than N_γ^{AV}, though these bounds are the best obtained using this technique. This is consistent with these solutions being rigorous upper bounds. The estimates provided by Zhu et al. (2001) using the third scheme (N_γ minimum) seems to agree well with N_γ^{AV} for low friction angles, where the shape of the rigid wedge has less effect. The numerical values suggested by Bolton and Lau (1993)

are inaccurate for the rough footing case and are higher than Michałowski's results. This is probably due to the assumption of a triangular wedge in their analysis. Bolton and Lau's (1993) results for a smooth footing are in excellent agreement with our numerical results. This is because their assumed failure mechanism, which is of the Hill type, closely models the correct failure mechanism. Further, the extent of Hill's mechanism is considerably smaller, so that the assumption of a straight edge does not affect the result for N_γ. The results obtained by Kumar (2003) agree very well with N_γ^{AV} for a rough footing, except for low friction angles. This could be due to the effect of the small surcharge that is needed to solve their system of equations. Again, the analytical expression provided by Poulos et al. (2001) appears to be in good agreement with N_γ^{AV} for most values of the friction angle except for very low/high friction angles where it overestimates/underestimates N_γ^{AV}. The closeness of the estimates given by $(34)_2$ to N_γ^{AV} suggests that the Booker (1969) solution is probably quite close to the exact solution. The results for displacement-based finite element and finite difference calculations presented by Frydman and Burd (1997) are found to be very conservative for $\phi > 30°$.

7. Conclusions

This paper presents rigorous and accurate estimations for the bearing capacity factor N_γ for rough and smooth rigid strip footings. The error bounds do not exceed 3.42%. Based on the numerical results obtained, a new approximate expression for the bearing capacity factor N_γ is proposed. This new formula is simple to use and provides accurate values. It is shown that some well-known solutions can overestimate N_γ significantly, and that the roughness of the soil-footing interface has a profound effect. This is explained by observing that a Prandtl-type failure mechanism is associated with a rough footing while the Hill mechanism, which is smaller, correctly models a smooth footing. In agreement with solutions obtained by the slip-line method, the predicted failure mechanisms show a curved rigid-wedge for a rough foundation and a curved wedges for a smooth foundation.

References

Abbo, A.J., Sloan, S.W., 1995. A smooth hyperbolic approximation to the Mohr–Coulomb yield criterion. Computers and Structures 54 (3), 427–441.

Bishop, J.F.M., 1953. On the complete solution to problems of deformation of a plastic rigid material. Journal of the Mechanics and Physics of Solids 2 (1), 42–53.

Bolton, M.D., Lau, C.K., 1993. Vertical bearing capacity factors for circular and strip footings on Mohr–Coulomb soil. Canadian Geotechnical Journal 30 (6), 1024–1033.

Booker, J.R., 1969. Applications of Theories of Plasticity to Cohesive Frictional Soils. PhD thesis, Sydney University.

Caquot, A., Kérisel, J., 1953. Sur le terme de surface dans le calcul des fondations en milieu pulvérulents. In: Proceedings of the Third International conference on Soil Mechanics and Foundation Engineering, Zürich, pp. 336–337.

Chen, W.F., 1975. Limit Analysis and Soil Plasticity. Elsevier, Amsterdam.

Davis, E.H., Booker, J.R., 1971. The bearing capacity of strip footings from the standpoint of plasticity theory. In: Proceedings of the first Australian–New Zealand Conference on Geomechanics, Melbourne, pp. 275–282.

Day, R.A., Potts, D.M., 2000. Discussion of "Observations on the computation of the bearing capacity factor N_γ by finite elements" by P.K. Woodward and D.V. Griffith. Géotechnique 50 (3), 301–303.

Drescher, A., Detournay, E., 1993. Limit load in translational failure mechanism for associative and non-associative materials. Géotechnique 43 (3), 443–456.

Drucker, D.C., Greenberg, W., Prager, W., 1952. Extended limit design theorems for continuous media. Quarterly Journal of Applied Mathematics 9, 381–389.

Frydman, S., Burd, H.J., 1997. Numerical studies of bearing-capacity factor N_γ. Journal of Geotechnical and Geoenvironmental Engineering 123 (1), 20–29.

Griffiths, D.V., 1982. Computation of bearing capacity factors using finite elements. Géotechnique 32 (3), 195–202.

Hansen, J.B., 1970. A revised and extended formula for bearing capacity. Bulletin of the Danish Geotechnical Institute 28, 5–11.
Hansen, B., Christensen, N.H., 1969. Discussion of "Theoretical bearing capacity of very shallow footings" by A.L. Larkin. Journal of Soil Mechanics and Foundations Division (ASCE) 95 (SM6), 1567–1568.
Hill, R., 1949. The plastic yielding of notched bars under tension. Quarterly Journal of Applied Mathematics 2, 40–52.
Hjiaj, M., Lyamin, A.V., Sloan, S.W., 2003. Calculation of the N_γ bearing capacity factor by F.E. limit analysis. In: Proceedings of the Seventh International Conference on Computational Plasticity (COMPLAS 2003). CIMNE, Barcelona, Spain.
Kármán, Th.v., 1926. Über elastische Grenzzüstande. In: Proceedings of the Second International Congress for Applied Mechanics, Zürich.
Kumar, J., 2003. N_γ for rough strip footing using the method of characterisitics. Canadian Geotechnical Journal 40 (3), 669–674.
Kumbhojkar, A.S., 1993. Numerical evaluation of Therzaghi's N_γ. ASCE Journal of Geotechnical Engineering 119 (3), 598–607.
Larkin, L.A., 1968. Total bearing capacity of very shallow footings. Journal of Soil Mechanics and Foundations Division (ASCE) 94 (SM6), 1347–1357.
Lundgren, H., Mortensen, K., 1953. Determination by the theory of plasticity of the bearing capacity of continuous footings on sand. In: Proceedings of the Third International Conference on Soil Mechanics and Foundation Engineering, Zürich, Switzerland, pp. 409–412.
Lyamin, A.V., Sloan, S.W., 2002a. Upper bound limit analysis using linear finite elements and nonlinear programming. International Journal for Numerical and Analytical Methods in Geomechanics 26 (2), 181–216.
Lyamin, A.V., Sloan, S.W., 2002b. Lower bound limit analysis using linear finite elements and nonlinear programming. International Journal for Numerical Methods in Engineering 55 (5), 573–611.
Manoharan, N., Dasgupta, S.P., 1995. Bearing capacity of surface footings by finite elements. Computers and Structures 54 (4), 563–586.
Meyerhof, G.G., 1951. The ultimate bearing capacity of foundations. Géotechnique 2 (4), 301–332.
Meyerhof, G.G., 1963. Some recent research on the bearing capacity of foundations. Canadian Geotechnical Journal 1 (1), 16–26.
Michałowski, R.L., 1997. An estimate of the influence of soil weight on bearing capacity using limit analysis. Soils and Foundations 37 (4), 57–64.
Nagtegaal, J.C., Parks, D.M., Rice, J.R., 1974. On numerically accurate finite element solutions in the fully plastic range. Computer Methods in Applied Mechanics and Engineering 4 (2), 153–177.
Poulos, H.G., Carter, J.P., Small, J.C., 2001. Foundations and retaining structures–research and practice. In: Proc. 15th International Conference on Soil Mechanics and Foundation Engineering, Istanbul, Turkey, vol. 4. A.A. Balkema, Rotterdam, pp. 2527–2606.
Prandtl, L., 1921. Über die Eindringungs-festigkeit (Härte) plastischer Baustoffe und die Festigkeit von Schneiden. Zeitschrift für Angewandte Mathematik und Mechanik 1 (1), 15–20.
Reissner, H., 1924. Zum Erddruckproblem. In: Biezend, C.B., Burgers, J.M. (Eds.), Proc. First Congr. Appl. Mech., pp. 295–311.
Sloan, S.W., 1988. Lower bound limit analysis using finite elements and linear programming. International Journal for Numerical and Analytical Methods in Geomechanics 12 (8), 61–77.
Sloan, S.W., 1989. Upper bound limit analysis using finite elements and linear programming. International Journal for Numerical and Analytical Methods in Geomechanics 13 (8), 263–282.
Sloan, S.W., Kleeman, P.W., 1995. Upper bound limit analysis with discontinuous velocity fields. Computer Methods in Applied Mechanics and Engineering 127, 293–314.
Sloan, S.W., Randolph, M.F., 1982. Numerical prediction of collapse loads using finite element methods. International Journal for Numerical and Analytical Methods in Geomechanics 6 (1), 47–76.
Sokolovskii, V.V., 1965. Statics of Soil Media. Pergamon Press.
Soubra, A.-H., 1998. Upper-bound solutions for bearing capacity of foundations. Journal of Geotechnical and Geoenvironmental Engineering 125 (1), 59–68.
Terzaghi, K., 1943. Theoretical Soil Mechanics. John Wiley & Sons, New York.
Ukritchon, B., Whittle, A.W., Klangvijit, C., 2003. Calculations of bearing capacity factor N_γ using numerical limit analyses. Journal of Geotechnical and Geoenvironmental Engineering 129 (6), 468–474.
Vesić, A., 1975. Bearing capacity of shallow foundations. In: Winterkorn, H.F., Fang, H.Y. (Eds.), Foundation Engineering Handbook. Van Nostrand Reinhold, New York, pp. 121–147.
Wang, Y.-J., Yin, J.-H., Chen, Z.-Y., 2001. Calculation of bearing capacity of a strip footing using an upper bound method. International Journal for Numerical and Analytical Methods in Geomechanics 25 (8), 841–851.
Woodward, P.K., Griffiths, D.V., 1998. Observations on the computation of the bearing capacity factor N_γ by finite elements. Géotechnique 48 (1), 137–141.
Zienkiewicz, O.C., Cormeau, I.C., 1974. Viscoplasticity, plasticity and creep in elastic solids. A unified numerical approach. International Journal for Numerical Methods in Engineering 8 (4), 821–845.
Zhu, D., 2000. The least upper-bound solution for the bearing capacity factor N_γ. Soils and Foundations 40 (1), 123–129.
Zhu, D.Y., Lee, C.F., Jiang, H.D., 2001. A Numerical study of the bearing capacity factor N_γ. Canadian Geotechnical Journal 38 (1), 1090–1096.